RSC Advances

ROYAL SOCIETY OF CHEMISTRY

www.rsc.org/advances

Journal Name

ARTICLE

Effects of functional group on the tribological properties of hairy silica nanoparticles as an additive to polyalphaolefin

Received 00th January 20xx,
Accepted 00th January 20xx

DOI: 10.1039/x0xx00000x

www.rsc.org/

Tianyi Sui, Baoyu Song* Feng Zhang and Qingxiang Yang

Hairy nanoparticles, which combine inorganic nanoparticles and organic polymers, have led to a variety of applications due to their special properties. In this paper, hairy silica nanoparticles (HSNs) with different functional groups were prepared and tested with their tribological properties as additives to polyalphaolefin (PAO). Unmodified silica nanoparticles were synthesized by stöber method and then modified by silanes with amino functional groups. The end groups of silica nanoparticles were further functionalized by tethering different organic chains to the amino functionalized HSNs. HSNs-PAO lubricants were prepared by a four-step process and tested with their tribological performances using a four-ball tribometer. The coefficient of friction was recorded and the wear scar surfaces were examined by SEM and EDS. It was found that HSNs could form stable homogenous solution when disperse in PAO and exhibited good anti-wear and friction reduction properties. NH2 terminated HSNs exhibited the best tribological performance but more concentration sensitive than other types of HSNs due to the hydrogen bond between amino groups. The long wear test result suggested that HSNs with Polar functional groups accelerate the running-in process, which could be attributed to the adsorption of HSNs.

1. Introduction

Hairy nanoparticles, which the nanoparticles were covered with organic coronas, are widely researched during the last two decades. With the organic chains on the surface of nanoparticles, the dispersion of nanoparticles in organic solvents was greatly improved. Additionally, functional groups on organic chains of hairy nanoparticles changed the properties of nanoparticles and provided various possibilities for applications of nanoparticles in various fields such as electrical,[1] medical,[2] optical[3] and mechanical fields.[4] As the organic coronas could enhance the dispersity and stability of nanoparticles in lubricants, the applications of hairy nanoparticles in tribological fields is of special interest. Different kinds of nanoparticles were investigated on their tribological properties such as ZrO_2,[5] $CaCO_3$,[6] TiO_2,[7] Al_2O_3[8] and Carbon.[9,10] Among those nanoparticles, hairy silica nanoparticles (HSNs) were one of the best nanoparticles for tribological applications as their environmental friendly and economic efficient properties. Hairy silica nanoparticles were prepared and investigated with their tribological properties.[11-16] Although HSNs exhibited good anti-wear and friction reduction performances, HSNs with different functional groups show different tribological properties. Most researchers focus on one type of functional groups when study the tribological properties of HSNs. Thus, the effects of different functional groups on the tribological properties of HSNs were still of great necessity to be further investigated.

Silica nanoparticles with amino functional groups were investigated on their tribological performances as additives in lubricants[11,12] and composites.[13] Those amino functionalized nanoparticles exhibited good dispersity and stability when filled into lubricants or composites, improved the tribological performance of lubricants and enhanced the mechanical properties. Amino functionalized thin film was also reported on good friction reduction performance, amino ligands with longer organic chains show lower friction coefficient due to the densely packed organic chains.[17] Despite that amino functionalized nanoparticles shows good tribological properties, the interparticle aggregation limited its applications. It was reported by R. Bagwe et al. that amino functionalized nanoparticles aggregated due to nonspecific bond between amino groups. Comparing with amino groups, carboxyl functional groups could prevent the nanoparticle agglomeration and enhance the stability of nanoparticles.[18] Beside good dispersity and stability, carboxyl groups were also reported for good corrosion resistance and frictional durability on metal evaporated tape.[19] Non-polar functional groups such as phenyl groups and long chain alkyl groups were also investigated on their tribological performances. R. Jones et al. reported that the phenyl groups could enhanced the life time of self-assembled monolayer and reduced the friction by forming a multicomponent film on the surface.[20] Y. Chen et al. studied the tribological performance of phenyl modified PTFE/Silica composite and found that the dielectric properties, wear absorptions and tensile strength were enhanced.[21] For alkyl groups, it was reported that nanoparticles with long alkyl chains could form homogeneous solution with base oil and exhibited good load carrying, anti-wear and friction reduction

[a] School of Mechatronics Engineering, Harbin Institute of Technology, Harbin, Heilongjiang, 150001, P.R.China. E-mail: sby@hit.edu.cn; Fax:+86-0451-86402016

properties,[22,23] long alkyl chains showed lower friction force and better anti-wear property than short chains.[24]

Keeping in view of the previous work reviewed above, different functional groups (amino,[11-13] carboxyl,[18,19] phenyl,[20,21] and alkyl[22-24] groups) were investigated with their tribological properties, functional groups directly affected the tribology properties of HSNs. However, most researchers studied on one type of functionalized nanoparticles and only a few of them focus on silica nanoparticles. The influence of functional groups on the tribological properties of hairy silica nanoparticles is still unclear. Thus, an investigation of the effect of functional groups on tribological properties of HSNs is needed to develop the understanding of the tribological properties of HSNs and extend the applications of them as potential additives in lubricants.

In this paper, a four-step method for preparing HSNs-PAO lubricants, including USNs synthesis, HSNs synthesis, solvent transfer and HSNs dispersion in lubricant, was developed. Prepared HSNs were characterized by several methods including scanning electron microscope (SEM), X-ray diffraction (XRD), Zeta potential, dynamic light scattering (DLS), Fourier Transform Infrared Spectroscopy (FTIR), X-ray diffraction and X-ray photoelectron spectra (XPS) and thermal gravity analysis (TGA). The viscosity-temperature dependence of the HSNs-PAO lubricants were investigated by Brookfield viscometer. The tribological performances of HSNs with different functional groups were tested using a four-ball tribometer. Coefficient of friction (COF) and wear scar diameter (WSD) for short and long time wear were measured. Base on the test result, optimal functional groups for HSNs were investigated. Different running-in performances of HSNs-PAO lubricants were found in the tribological test. It is suggested that adding HSNs into lubricant could reduce the duration of running-in process and stable COF. Meanwhile, HSNs with polar function groups would accelerate the running-in period. A three period running-in process was developed based on the test result, the mechanism of the anti-wear and friction reduction performance of HSNs were discussed.

2. Materials and Methods

2.1 Materials

The materials listed following were used as received: Tetraethylorthosilicate (TEOS, 99% purity, Sinopharm), ammonium hydroxide (28% purity, Sinopharm), ethanol (99% purity, Sinopharm)toluene(99% purity, Sinopharm), N1-(3-Trimethoxysilylpropyl)diethylene-triamine (DETAS, 95% purity, Sigma Aldrich), stearic acid (STA, 90% purity, Sinopharm), benzoic acid(BEA, 99% purity, Sinopharm), succinic acid(SUA, 99%, Sinopharm), polyalphaolefin (PAO, 99% purity, fox chemical technology).

2.2 Preparation of HSNs-PAO lubricants

Unmodified silica nanoparticles were prepared before modification. 100nm silica nanoparticles were prepared by stöber method. TEOS was first diluted with ethanol and then added into the mixture of ethanol, water and aqueous ammonia with gently stirred at temperature of 40 ℃ for 3 hours. As shown in Fig. 1 (a), a transparent solution with light blue colour was obtained after the reaction, which suggested that the silica

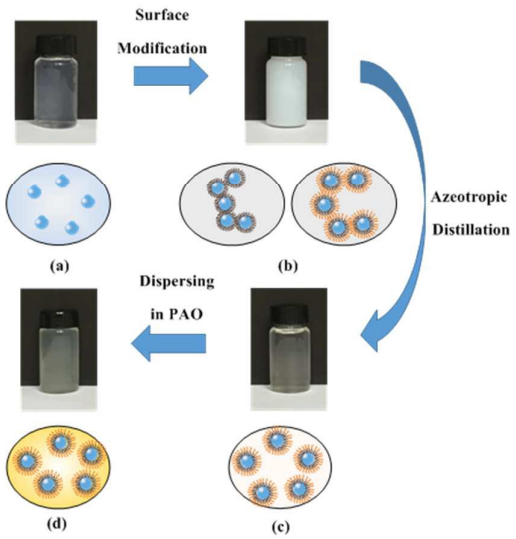

Fig. 1 The schematic diagram of HSN-PAO lubricant preparation process: (a) unmodified silica nanoparticles dispersed in ethanol, (b) HSNs dispersed in ethanol, (c) HSNs dispersed in toluene and (d) HSNs dispersed in PAO.

nanoparticles were mono-dispersed with narrow size distribution.

Silica nanoparticles prepared above were modified by DETAS. In order to densely graft organic chains onto silica nanoparticles, excess of silane was added into the silica nanoparticle solution drop by drop with rapid stirring. The solution was continuing heated at 50℃ for 12 hours to ensure the linking reaction finished. After the reaction, unlinked silane and impurities was removed by dialysis using 10,000 MWCO snakeskin dialysis tube obtained from Themoscientific. NH_2 terminated HSNs were obtained after the dialysis process finished. Those HSNs were covered with amino functional groups and could be further modified by acid-terminated organic chains.

In order to modify the ending functional group of HSNs, carboxyl-terminated organic chains were tethered to the amino functional group of NH_2 terminated HSNs synthesized above. STA, BA and SA were first dissolved in ethanol respectively then added into the NH_2 terminated HSNs solution drop by drop with rapid stirring, DCCI was taken as a dehydration agent for the formation of peptide bond between carboxyl group and amino group. The solution was kept stirring at room temperature for 12 hours to ensure the linking reaction finished. HSNs prepared above were purified again by filtration and dialysis to remove the impurities and unlinked organic chains. HSNs with carboxyl, phenyl and long-chain alkyl ending groups were obtained after the purification process finished. As shown in Fig. 1 (b), the solution turn white turbid after the surface modification reaction, which were due to the formation of micelles in the ethanol solution. The molecular

structures of different HSNs were shown in Fig. 2. The covalent siloxane bridges were created after the linking reaction between hydroxyl group and siloxane. The primary amino functional groups were further modified by tethering acid terminated organic chains to it.

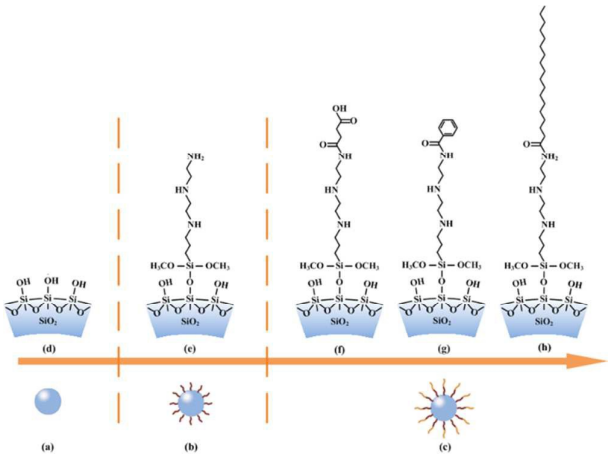

Fig. 2 Different types of silica nanoparticles: (a) unmodified silica nanoparticles (USNs), (b) hairy silica nanoparticles (HSNs) and (c) HSNs which were further functionalized by organic chains. Surface structure of (d) USNs, (e) NH_2 terminated HSNs, (f) COOH terminated HSNs (g) C_6H_5 terminated HSNs and (h) CH_3 terminated HSNs.

In order to disperse HSNs into PAO lubricant, HSNs were first transferred from ethanol to toluene by azeotropic distillation. Toluene was added into the HSNs-ethanol solution obtained above to form a 3/1 mixture of toluene and ethanol. The solution was kept at 70 ℃ for 3 hour to remove the ethanol. After the azeotropic distillation process, HSNs were transferred to toluene. PAO was then added into the solution with rapid stirring. The solution was then transferred to a convection oven to remove toluene from PAO.

2.3 characterization of hairy silica nanoparticles

The morphology of HSNs was characterized by a Hitachi SU8010 scanning electron microscope (SEM). Silica nanoparticles were treated with sputter-gold to enhance the conductivity before the experiment. The X-ray diffraction (XRD) patterns of silica nanoparticles (2ϑ = 5~90°)were recorded by Panalytical Empyrean X-ray diffractometer, using a Cu Kα radiation at 25℃ with a 2θ step size of 0.02 and a scanning speed of 2° /min. The Fourier Transform Infrared Spectroscopy (FTIR) of HSNs were examined by Nicolet IS10 with a spectra range of 400-4000 cm^{-1}. The XPS experiments were performed on a Thermo Fisher Scientific X-ray photoelectron spectroscopy 250Xi (Al Kα line of 1486.6 eV, energy and 120W), the ultra-high vacuum chamber analysis chamber were maintained at a typical base pressure of 5×10^{-9} Torr during sample analysis. The surface area of unmodified silica nanoparticles was characterized by Brunauer-Emmett Teller (BET) method and the nanoparticles were pre-treated under vacuum condition at 150 ℃ for 2 h before the BET test. Thermogravimetric analysis (TGA) was employed using a TA Q500 and heating at a rate of 10 ℃/min to 800 ℃ under flowing nitrogen gas. The Zeta potential and dynamic light scattering of HSNs were characterized by a Zetasizer Nano ZS from Malvern Instruments.

2.4 Tribological properties of hairy silica nanoparticles

The viscosity-temperature dependence for different types of HSNs-PAO lubricants were investigated by an Brookfield viscometer using a cone/plate tester, with the temperature range of 25℃~100. Tribological properties of HSNs-PAO lubricants were tested using a MRS-10 four-ball tribometer. The test apparatus and configuration was shown in Fig. S6. All test were performed at rotating speed of 1450r/min, under a load of 390N at room temperature. 12.7mm diameter GCr15 steel bearing balls (grade 4) were cleaned ultrasonically with ethanol before the test. COF and WSD of HSNs-PAO lubricants with different concentrations and functional groups were tested for 30 min for three times and average COF and WSD were calculated. Based on the results, HSNs with different functional groups were tested for 3h at their best concentration to investigate the running-in period and anti-wear performance under long-wear condition. The wear surfaces of steel bearing ball after the tribology test were examined by SEM and EDS. Before the SEM and EDS test, the steel bearing ball were rinsed in ethanol for 5 minutes using ultrasonication and dried in vacuum drying oven.

3. RESULT AND DISCUSSION

3.1 Hairy silica nanoparticle Characterization

The morphology of Silica nanoparticles were characterized by SEM. As shown in Fig. 3 (a), 100nm silica nanoparticles were prepared successfully by stöber method, with excellent roundness and narrow size distribution. NH_2 terminated HSNs were synthesized by modifying USNs with DETAS. The SEM of NH_2 terminated HSNs were shown in Fig. 3 (b), large cluster of HSNs were found at high concentrations (10 wt %) of NH_2 terminated HSNs, which could be due to the hydrogen bond between amino functional groups.[18] Comparing with NH_2 terminated HSNs, functionalized HSNs which further modified by organic chains show better dispersity at both high and low concentrations. Fig. 3 (c) and (d) show the CH_3 terminated HSNs at high concentration (10 wt %) and low concentration (0.5 wt %) respectively. CH_3 terminated HSNs did not aggregate or form large cluster but kept well dispersed at both low (0.5 wt %) and high (10 wt %) concentration. Silica nanoparticles were further characterized by X-ray diffraction (XRD). The XRD pattern (Fig S1) of both USNs and HSNs exhibited broad peaks at 22°, 31.3° and

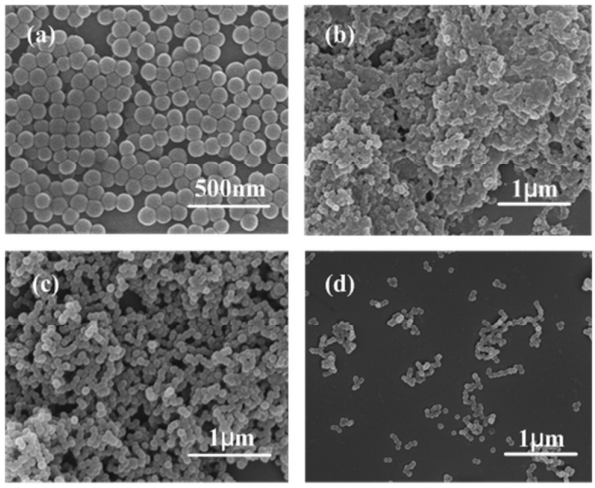

Fig. 3 SEM micrograph of (a) 100 nm USNs, (b) NH2 terminated HSNs, (c, d) CH3 terminated HSNs at high concentration (10wt %) and low concentration (0.5 wt %).

36° 2ϑ, which are the characteristic of silicon. It could be found from XRD patterns and SEM micrographs that silica nanoparticles remain their structural and size integrity after the modification.

The HSNs were characterized by FTIR and the spectra were shown in Fig. 4. All kinds of HSNs show a strong band at 1010-1100 cm^{-1}, which is the Si-O-Si stretching vibration. A broad band at 3300 cm^{-1} were found for USNs, corresponds to O-H stretching. Peak at 1620cm^{-1} for the spectrum of NH_2, 1550 cm^{-1} for CH_3, 1555cm^{-1} for COOH and 1552 cm^{-1} for C_6H_5 corresponds to the N-H bending. A broad band at 3400 cm^{-1} for NH_2 could be assigned to H–bonded N-H stretching. A peak at 1723 cm^{-1} and a broad band at 3300 cm^{-1} were found in the spectrum of COOH, which corresponding to the C=O stretching and O-H stretching. The peak appears at 1454 cm^{-1} and 1600 cm^{-1} of C_6H_5 spectrum are the characteristics of the phenyl group while the peak at 2858 cm^{-1} and 2917 cm^{-1} of CH_3 spectrum are corresponding to the C-H stretching of alkane group.

The functionalized HSNs were further characterized by XPS, the XPS survey spectrum for USNs, NH2 terminated HSNs and CH3 terminated HSNs were shown in Fig. 5 (a, b and c). It could be found from the XPS survey spectrum that Si2p at 101.1 eV and O1s at 543.7 eV were found in the spectra of USNs. After modified with amino functionalized silanes, an N1s peak at 397.5 eV emerged, which indicated that amino functional groups were successfully introduced on silica nanoparticle surface. With further functionalized by long alkyl chain, the peak area of C1s increase for 30% while the peak area of N1s remain the same. The deconvoluted C1s subregion for NH2 terminated, COOH terminated, C6H5 terminated and CH3 terminated HSNs were shown in Fig. 5 (d, e, f and g). As shown in Fig. 5 (d), the XPS spectrum of C1s could be deconvoluted into three Gaussian peaks, which are typical peak of C-Si peak at 282.7 eV, C-H peak at 283.9 eV and C-C peak at 284.6 eV. After functionalized by carboxyl groups, three new peak emerged, which are C-O peak at 285.8, C=O peak at 287.1 and O-C=O peak at 288.9. The C1s subregion for C6H5 terminated HSNs was deconvoluted into four peaks, corresponding to C-H peak at 283.8 eV and C-C peak at 284.6 eV, and C6H5 peak at 286.2. The spectra for CH3 terminated HSNs was deconvoluted into three peaks, which are C-Si peak at 282.9 eV, C-H peak at 283.8 eV and C-C peak at 284.6 eV. It could be conclude from the experiment result that functional groups were introduced on the surface of silica nanoparticles successfully.

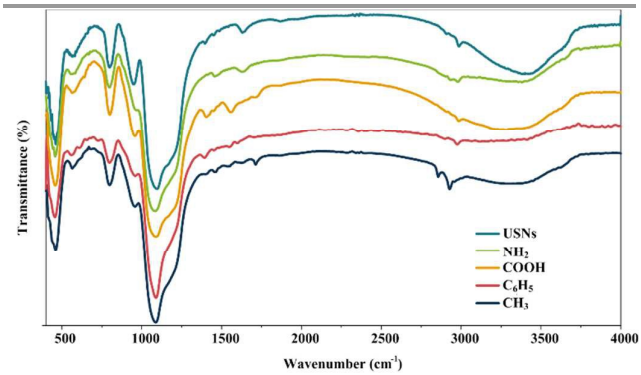

Fig. 4 The FTIR spectra of HSNs with different functional groups

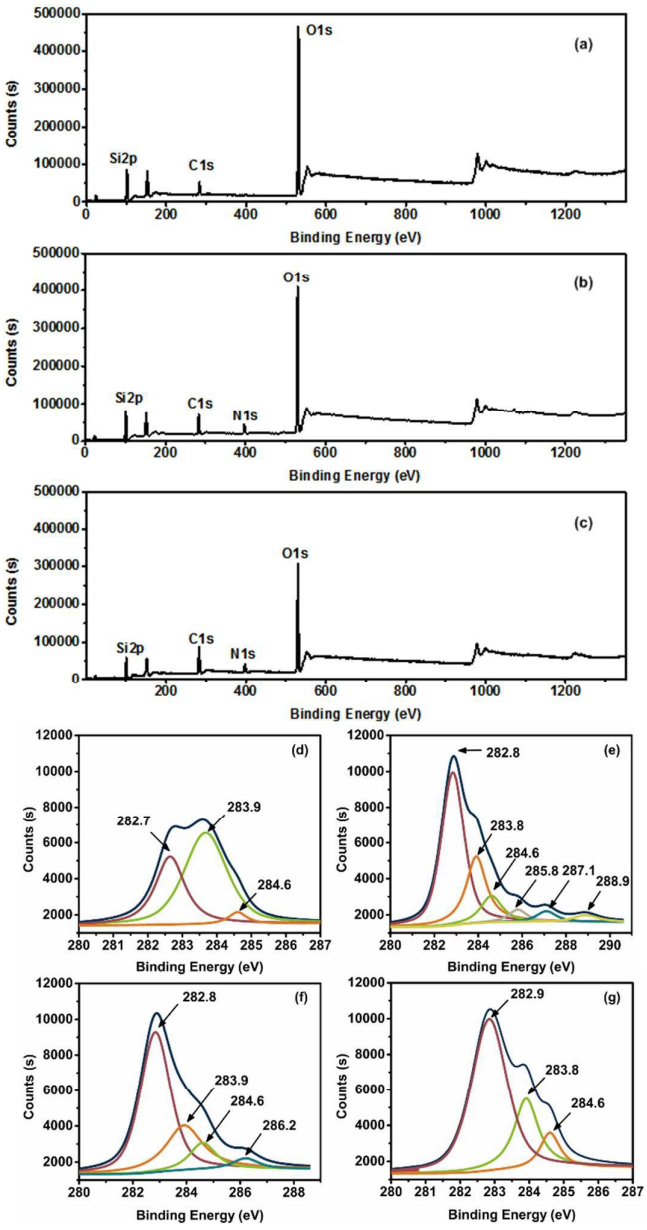

Fig. 5 The XPS survey spectra of (a) USNs, (b) NH2 terminated HSNs and (c) CH3 terminated HSNs, deconvoluted C1s subregions of (d) NH2 terminated, (e) COOH terminated, (f) C6H5 terminated and (g) CH3 terminated HSNs and HSNs.

The organic content of HSNs was quantified by TGA method. HSNs with different organic chains were heated from room temperature to 800 ℃ at heating rate of 10 ℃/min, the result was shown in Fig. 6. It could be found from the graph that all four TGA curves show same trends, which organic chains start to degrade around 300 ℃, and fully degraded around 600 ℃ while the inorganic silica core would remain at the end of the test. The surface area of unmodified silica nanoparticles was tested with BET method and the surface area was 271 m^2/g. Based on the BET and TGA test result. The grafting density of HSNs was 1.1~ 1.3 ligand/nm^2.

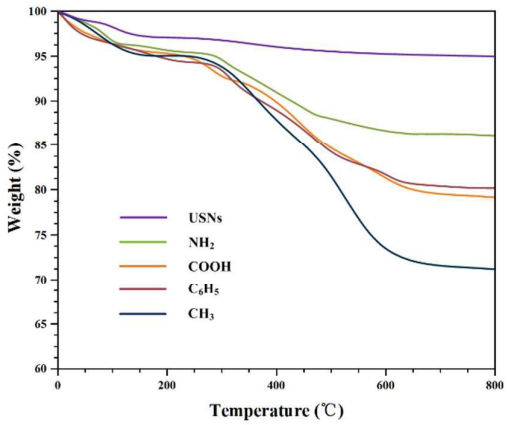

Fig. 6 Thermogravimetric analysis of HSNs with different functional groups

The Zeta potential of silica nanoparticles dispersed in ethanol were characterized by a Malvern Zetasizer Nano ZS. Zeta potential value for USNs was observed at -42 mV, which was due to abundant hydroxyl groups on the surface of silica nanoparticles. After modified with amino functionalized silanes, the zeta potential increased to +27 mV, which could be attributed to the primary amino groups on the surface of HSNs. The change of zeta potential value confirmed that the amino functional groups were successfully introduced onto the surface of silica nanoparticles. The zeta potential value decreased to about +21~+24 mV after further functionalization of silica nanoparticles (Fig. S3). Which could be due to the transfer from primary amino groups to secondary amino groups.

The long-term stability of HSNs-PAO lubricants was studied by keeping the lubricants standing for 2 months after the preparation process finished. The photograph of different kinds of lubricants are shown in Fig. 7. Four kinds of HSNs-PAO lubricants prepared by the four-step process introduced in this paper are shown in Fig. 7 (a, b, c, and d) and two kind of HSNs-PAO lubricants prepared by common method are shown in Fig. 7 (e and f) respectively. It could be found that HSNs form homogenous solution with PAO lubricants and keep stable after 2 months standing. CH_3 (shown in Fig.7 (a)) and C_6H_5 (shown in Fig. 7 (b)) terminated HSNs show better optical transparency than COOH and NH_2 terminated HSNs, which could be attributed to excellent compatibility of the non-polar functional groups in organic solvent. Fig. 7 (e) shows USNs dispersed in PAO and Fig. 7 (f) shows NH_2 terminated HSNs dispersed in PAO using common method which dries HSNs to powder after the preparation, then redisperse them into lubricant by stirring or ultrasonic dispersion. Comparing with Fig. 7 (d) which the same kind of HSNs dispersed in PAO by four step process, HSNs dispersed by common method partly sedimented on the bottom after 2 month standing, which suggested HSNs dispersed by common method has worse stability than HSNs dispersed by four-step process. Meanwhile, as shown in Fig. 7 (e), USNs dispersed in PAO completely sedimented on bottom of the bottle after 2 month standing, which show the worst stability among all kinds of lubricants shown in Fig. 7. It could be found from the long-term stability test that HSNs dispersed

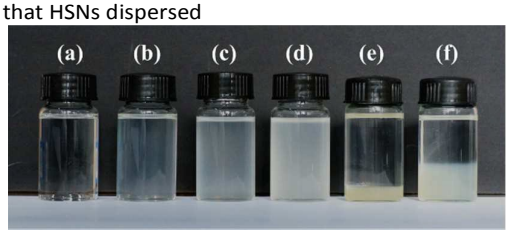

Fig. 7 Photograph of PAO with (a) CH_3 terminated HSNs, (b) C_6H_5 terminated HSNs, (c) COOH terminated HSNs and (d) NH_2 terminated HSNs prepared by four-step process, PAO with (e) USNs and (f) NH_2 terminated HSNs dispersed by common method.

by the four-step process formed homogeneous solution with PAO and exhibited excellent stability. This point is confirmed by DLS test (Fig. 8) that the average particle size of HSNs in PAO only increase slightly after 2 month standing. Keeping in view of the four-step process from synthesis of HSNs to dispersion in PAO, nanoparticles were kept dispersed in solutions (Ethanol, toluene and PAO) during the preparation of HSNs-PAO lubricant. Comparing with the commonly used process which dry the nanoparticles before dispersing them into lubricants, the new process increased the stability of HSNs while avoid the oxidation of HSNs during the drying process.

The dispersity and stability of HSNs were also studied by characterizing nanoparticle size of HSNs dispersing in ethanol and PAO using dynamic light scattering. The result was shown in Fig. 8. The average particle size of unmodified silica nanoparticles in ethanol was 102.1 nm. After modified with amino functionalized silane, the average nanoparticle size increased to 356.3 nm, indicated the aggregation of primary HSNs. With further functionalized by carboxyl, phenyl and alkyl chains, the nanoparticle size increase slightly for 20~40 nm. However, when transferred HSNs from ethanol to toluene, the average particle size of HSNs decreases sharply to 170~270nm, which indicated the high dispersion of HSNs in nonpolar medium. After transfer from toluene to PAO lubricant, the average particle size of HSNs increase slightly and after 2 month standing, the average particle size only increase for tens of nanometre. It could be found from the result that HSNs didn't disperse well in ethanol but when transferring into non-

polar solvent, the dispersion of HSNs improved significantly. Among

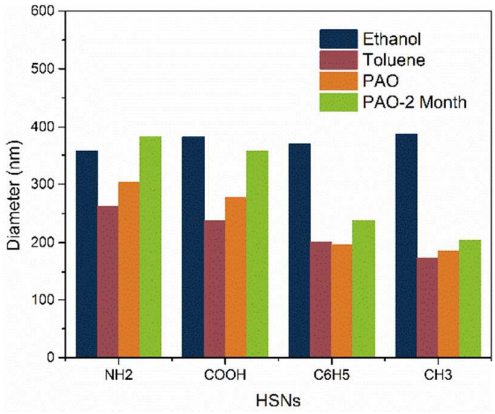

Fig.8 The average particle size of HSNs dispersing in ethanol, toluene and PAO (orange column is the average particle size of HSNs just after the dispersion and the green column is the particle size after HSNs-PAO standing for 2-month)

those HSNs, CH3 terminated HSNs perform the smallest average particle size and best stability when dispersing into PAO, which implied the best compatibility between nanoparticles and lubricant. NH2 and COOH terminated HSNs were found to have larger average particle size and the particle size increase more after 2 months standing than other types of HSNs, which indicates easier aggregation when dispersing in PAO.

3.2 Tribology properties of hairy silica nanoparticles

The viscosity of pure PAO and HSNs-PAO lubricants were tested using a cone-plate rheometer tester. The viscosity as a function of HSNs concentration and temperature were shown in Fig. S4 and Fig. S5 respectively. It could be found from the figure that with the increase of HSNs concentration, the viscosity of HSNs-PAO lubricants increased. NH2 and COOH terminated HSNs exhibited higher viscosity and increase rate than other HSNs (the viscosity of HSNs-PAO lubricant increase for 80% at concentration of 4%) while CH3 terminated HSNs exhibited the lowest viscosity (the viscosity of HSNs-PAO lubricant increase for 20% at concentration of 4%) among all kinds of HSNs. From Fig. S5, all kinds of HSNs shows good viscosity-temperature properties, the viscosity index of PAO lubricant increased for 3% after adding the HSNs into it (see Supporting Information).

The COF and WSD of different concentrations of HSNs with different functional groups were shown in Fig. 9. Comparing with the PAO lubricants without HSNs, all types of HSNs exhibited good anti-wear and friction reduction properties when adding into PAO with appropriate concentrations. Comparing with the COF and WSD of pure PAO without HSNs, which was 0.093 and 870μm, the COF and WSD of HSNs-PAO reduced optimally 40%. It could be found from the graph that amino functionalized nanoparticles show the best friction reduction and anti-wear properties (when concentration was at 1 wt%, COF was 0.055, WSD was 301μm) among all types of HSNs. That could be attributed to the chelation effect of amino groups and hemilability of amine-metal bond,[25] which could enhance the interaction between HSNs and metal surfaces. With more HSNs adsorbed on metal surface, the protecting effect (forming protecting film on metal surface), rolling effect (preventing two surfaces from contacting) and polishing effect (improving the surface roughness by filling the nano-groove and polishing the nano-pump) would be improved. However the tribological performance of amino functionalized HSNs shows stronger concentration sensitive behaviour than other three types of HSNs, which the COF and WSD fluctuated drastically with the concentration. This phenomenon may be caused by the polarity of primary amino functional groups and hydrogen bond between those amino functional groups. With strong polarity, the compatibility of amino functionalized HSNs with PAO lubricants would not as good as other three types of HSNs. Meanwhile, amino functionalized HSNs would attract each other and form large clusters by hydrogen bonds, which would cause three-body abrasion wear. As shown in Fig.3 (b), the NH_2 terminated HSNs would form large cluster at high concentration. Hydrogen bond between amino groups would give rise to aggregation of the nanoparticles, which might lead to partly uneven distribution at low concentration (0.5%) while form

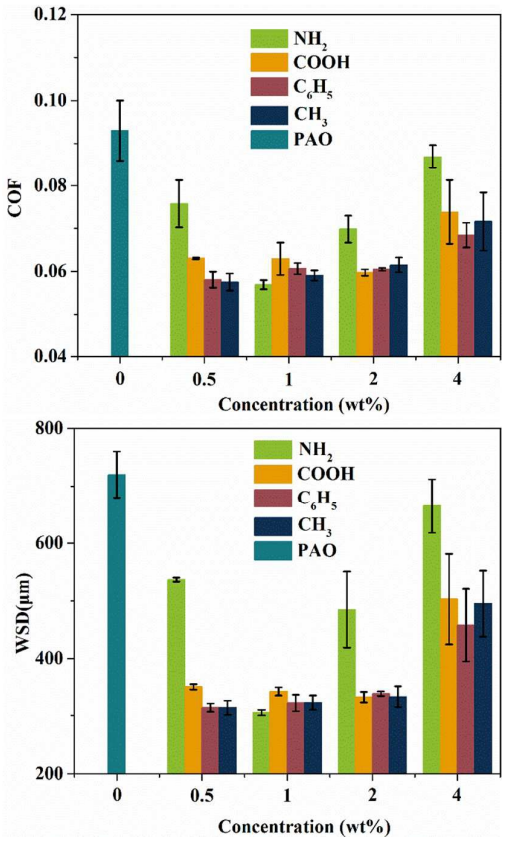

Fig. 9 The COF and WSD of HSNs with different functional groups

large cluster of nanoparticles and cause three body abrasion at high concentration (2% and 4%). As a result, insufficient or excess amount of amino functionalized HSNs would cause wear damage and increase the COF. COOH terminated HSNs shows worse anti-wear and friction reduction performance,

which might be due to the corrosive effect of acid functional groups. With further modified by the organic chains, the COF and WSD of HSNs become less concentration sensitive, which may be attributed to the longer organic chains and less polarity. With longer organic chains and less primary amino functional groups, the dispersity and stability of C_6H5 and CH_3 terminated HSNs were enhanced dramatically, meanwhile, with the nonpolar functional groups, HSNs became easier to form homogenous stable solution when dispersed into PAO lubricants.

The COF versus time for HSNs with different functional groups were shown in Fig. 10. It could be found from the figure that all the COF shows similar trend: a remarkable increase of COF could be found after a period of smooth running, which is the start of running-in period. When new equipment was running the first time, the moving parts would wear against each other severely until they settle into a stable condition. HSNs with different functional groups show different running-in performances: The COF of Pure PAO rose up dramatically at 1900s and became stable at 0.11 around 6000s. Comparing with pure PAO without HSNs, all types of HSNs-PAO lubricants show shorter duration in running in stage and lower steady state COF. The COOH terminated HSNs shows the highest peak value and longest duration time among four kinds of HSNs (the COF of COOH terminated HSNs increased to 0.095 around 3600s and became stable at 5400s). With an acidic ending group, the COOH terminated HSNs might react with metal surface and cause corrosion during the formation of transfer film. That would lead to an unstable development of the transfer film and result in longer and unstable duration time of running in period. The COF of NH_2 terminated HSNs exhibited the lowest stable COF, which could be attributed to the more adsorption of HSNs nanoparticles on the metal surface. Under the effect of physical adsorption (chelation effect and polar adsorption of amino group) and chemical adsorption (the hemilability of amine-metal bond), more HSNs were adsorbed on the metal surface so that the anti-wear and friction reduction properties of HSNs were enhanced. C_6H_5 and CH_3 terminated HSNs show the short running in durations and smooth stable period, which could be due to the better dispersity in PAO. With the non-polar group, C_6H_5 and CH_3 terminated HSNs would dispersed better than polar group terminated HSNs in PAO, which could prevent the aggregation more effectively and reduce the three body abrasion caused by large cluster of aggregated HSNs.

It could be found from the test result that the COF of HSNs-PAO lubricants shows the similar trend which the COF decrease slightly at first and interrupted with a dramatically increase, following with a quick decrease. After that the COF would remain stable. The schematic diagram of running-in process was shown in Fig. 11. When counterparts sliding against each other under the lubrication of HSNs-PAO, the HSNs would first polish the micro-bump and filled into the micro-grooves on the metal surface. That would improve the surface roughness of two counterparts, as a result, the COF would goes down slightly at the first period. This point is confirmed by the SEM micrograph (Fig. 12(c)). This period is the pre-running-in period. With the increasing numbers of HSNs adsorbed on the metal surface, some HSNs would interact with the surface, leading to surface oxidation, passivation and formation of transfer film. This process would cause wear and generate heat in the contact area. The COF would increase dramatically in this period. After the formation process of the protecting film, metal surface was covered with the protecting film including adsorbed layer and

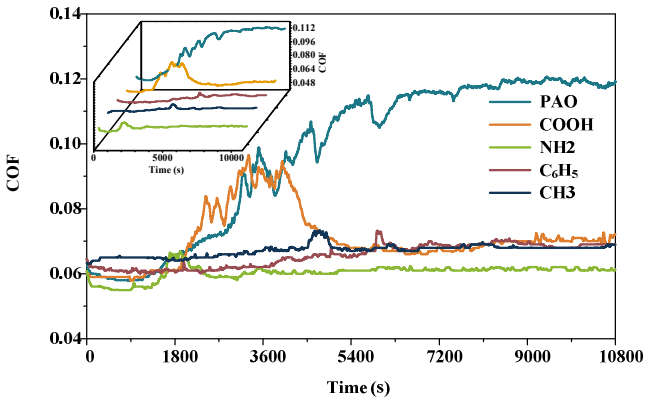

Fig. 10 COF versus time for different HSNs

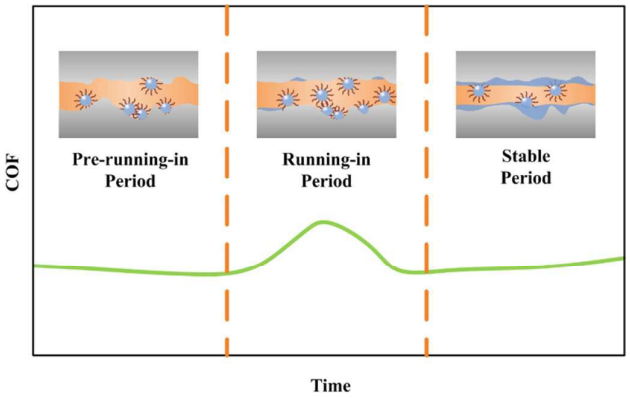

Fig. 11 Schematic diagram of running-in process including: (a) pre-running-in period, (b) running-in period and (c) stable period.

chemical reacted layer. The wear rate and COF would decrease under the protection of the transfer film. Although the protecting film would be removed and reformed on small scale of the metal surface when debris and micro bumps passed by, the surface would be generally covered with the protecting film and the COF would keep stable in the following period. This was confirmed in Fig. 12 (e and f), which the both cracking and new formed protecting layer were found on the protecting film.

It should be noted here that an interesting running-in period shift were found which polar groups (NH_2 and COOH) terminated HSNs would transfer from pre-running-in period to running-in period earlier than non-polar groups (CH_3 and C_6H_5). As reported by Chang et al.[26] the solid lubricants with PTFE could form thicker transfer film, which result in a shorter running-in stage. Bosman et al.[27] reported that the

mechanically altered layer at the top of the bulk material has an important influence on the running-in period. In our research, different running-in period duration and period transfer time were found. With the polar groups, NH_2 and COOH terminated HSNs would have more opportunities to adsorb on the metal surface due to the chemical and physical and chemical adsorption of the ending groups, which would accelerate the period transfer. NH_2 terminated HSNs show the fastest period transfer among all types of HSNs. This might be attributed to the chelation effect of amino functional groups and the hemilability of amine-metal bond that enhance the adsorption of HSNs on metal surface.

In order to further investigate the tribological mechanism of HSNs, the wear surfaces was examined by SEM. Typical wear surfaces of steel ball during pre-running-in period and stable period are shown in Fig.12. Fig 12(a, b and c) show a typical wear surface during pre-running-in period (steel ball were tested in tribological experiment for 30 mins) at different magnification. Fig. 12(b) was the high-magnification micrograph of the marked region in Fig. 12(a) while Fig. 12(c) was the high-magnification micrograph of the marked region in Fig. 12(b). From Fig. 12 (a) and (b), micro-grooves and nano-grooves were found on the wear surface. When we magnify the nano-grooves, we found large amount of nanoparticles in the grooves. Comparing with the flat surface beside the nano-grooves which barely had nanoparticles on it, the nanoparticles were successfully filled into the grooves. This micrograph meet well with the analysis of the pre-running-in period that nanoparticles would fill into the grooves, which would improve the surface roughness and reduce the COF. However, as the wear surface was still under pre-running-in period, the groove is not fully filled with nanoparticles. With longer time, more nanoparticles would filled into grooves and protecting film would then generate on the wear surface. Fig 12. (d, e and f) show a typical wear surface after the running-in period, which the steel ball were tested for 120 min. Fig. 12(e) is the high-magnification of the marked region in Fig. 12(d) while Fig. 12(f) is the high magnification of marked region in Fig. 12(e). It could be found from Fig. 12(d) that large area of the protecting film was formed on the surface of steel ball, which occupied the most area of the micrograph. When we magnified the protecting film(shown in Fig. 12(e)), we found micro-cracking appeared on protecting film, which means the protecting film might be delaminate and removed by the friction. However, when the marked region of Fig. 12(e) were further magnified, we found some silica nanoparticles on the edge of the protecting film. As shown in Fig. 12(f), some of the nanoparticles were unbroken and just attached on the film while some of the nanoparticles were broken and in the process of forming the protecting film. This confirmed the analysis that in the stable period, the protecting film would be removed and reformed at the same time.

The wear surface of different kinds of HSNs were investigated by SEM and EDS. SEM and EDS of typical wear surfaces for NH_2, COOH, C_6H_5 and CH_3 terminated HSNs were shown in Fig. 13 (a,e), (b,f), (c,g) and (d,h) respectively. As can be seen from the figure, dark areas on the wear surface were found after 30 minutes wear, the NH_2 terminated HSNs shows even distributed grey areas while COOH terminated HSNs shows spotted dark grey areas. Meanwhile, C_6H_5 and CH_3 terminated HSNs shows lighter colour on the wear surfaces than NH_2 and COOH terminated HSNs. NH_2, C_6H_5 and CH_3 terminated HSNs showed smooth wear surface with shallow wear tracks while COOH terminated HSNs showed deep scratching line on the wear surface, which indicated that ploughing phenomenon occurred seriously on the surfaces. The wear surfaces were then characterized by EDS. It could be found from the figure that, beside high peak corresponding to Fe and Cr, the peak corresponding to Si was found around 2 keV. The dark area observed on the wear surface were found containing higher Si than light colour areas, which suggested that HSNs adsorbed on that area and formed chemical reaction layer. The wear surface of NH_2 and COOH terminated HSNs shows higher Si counts than C_6H_5 and CH_3 terminated HSNs, which meet well with the interpretation that polar group would lead to more silica nanoparticle adsorptions and thicker chemical reaction layer on the metal surface.

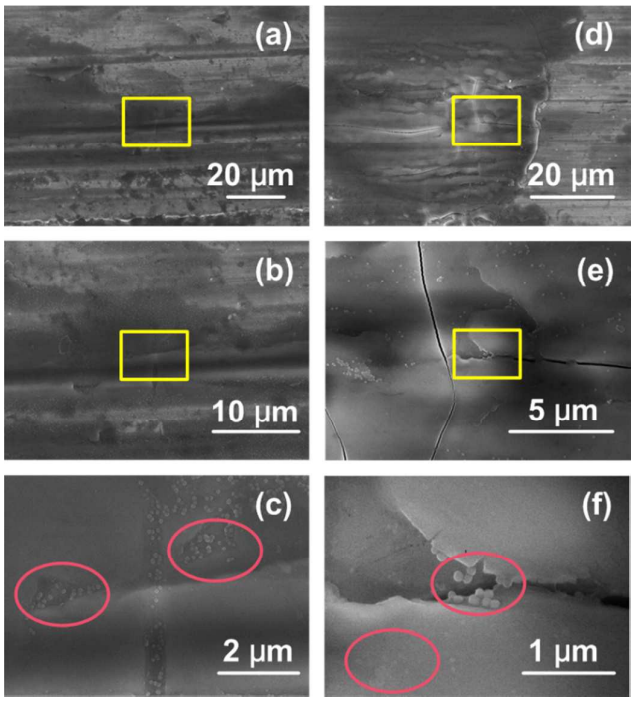

Fig. 12 The SEM micrograph of steel ball wear surface for pre-running-in period (a, b and c) and stable period (d, e and f). (b), (c), (e) and (f) are the high-magnification of marked regions in (a), (b), (d) and (e) respectively.

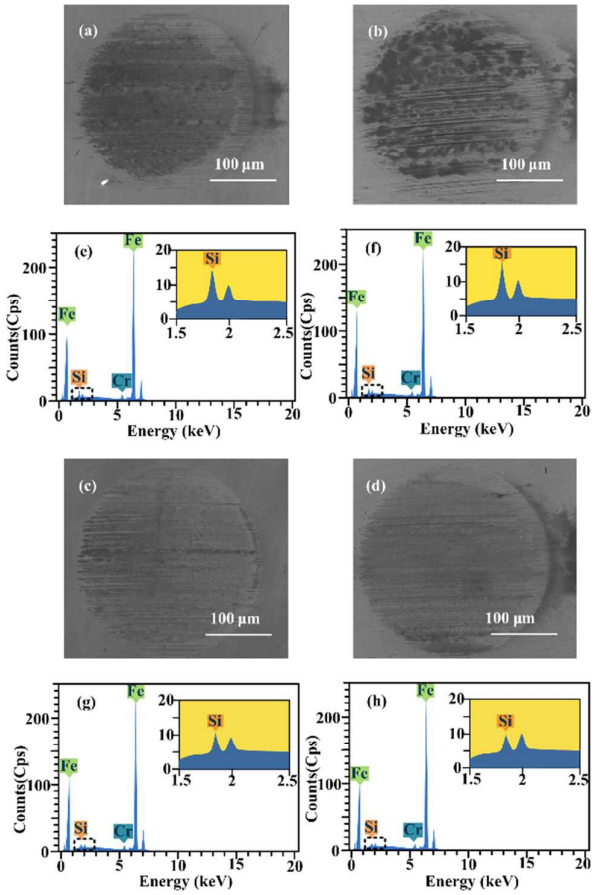

Fig. 13 The SEM and EDS of wear scar surfaces for different kinds of HSNs: (a, e) SEM and EDS for NH_2 terminated HSNs, (b, f) SEM and EDS for COOH terminated HSNs, (c, g) SEM and EDS for C_6H_5 terminated HSNs and (d, h) SEM and EDS for CH_3 terminated HSNs.

4 Conclusions

Hairy silica nanoparticles with four kinds of functional ending groups were synthesized and dispersed into PAO lubricants via a four-step process. HSNs were characterized by SEM, XRD, Zeta potential, DLS, XPS, TGA, BET and FTIR. The tribological properties of HSNs were characterized using a four-ball tribometer. Based on the test result, the effect of functional groups on the tribological properties of HSNs was discussed. It was found that NH_2 terminated HSNs exhibited the best anti-wear and friction-reduction properties due to the chemical and physical adsorption of NH_2 groups. However, NH_2 terminated shows concentration sensitive behaviour, which could be attributed to the hydrogen bond between primary NH_2 groups that cause aggregations. CH_3 and C_6H_5 terminated HSNs enhanced the stability of the tribological performance of HSNs, which could be due to the non-polar ending groups that increase the compatibility of HSNs in PAO lubricants. Moreover, a running-in phenomenon of HSNs-PAO lubricant was investigated, three different periods of the running-in phenomenon (pre-running-in period, running-in period and stable period) were proposed and discussed based on the experiment result. Nanoparticles would filled into the nano-grooves on wear surface and form protecting films during the running-in period. Polar functional groups (COOH and NH_2) terminated HSNs show more adsorption of HSNs on metal surface, which could lead to the acceleration of the running-in process.

Acknowledgements

The author would like to thank Prof. Donald Koch, Prof. Lynden Archer and Rahul Mangal, Chemical and Biological Engineering, Cornell University, for their helpful discussions and suggestions.

Notes and references

1 C. A. Grabowski, H. Koerner, S. Meth, A. Dang, C. M. Hui, K. Matyjaszewski, M. R. Bockstaller, M. F. Durstock and R. A. Vaia, *ACS Appl. Mater. Interfaces*, 2014, **6**, 21500–21509.
2 L. Casal-Dujat, M. Rodrigues, A. Yagüe, A. C. Calpena, D. B. Amabilino, J. Gonzaílez-Linares, M. Borraís and L. Peírez-Garciía, *Langmuir*, 2012, **28**, 2368–2381.
3 X. Lin, W.-L.-J. Hasi, X.-T. Lou, S. Lin, F. Yang, B.-S. Jia, D.-Y. Lin and Z.-W. Lu, *RSC Adv.*, 2014, **4**, 51315–51320.
4 K. Smaali, S. Desbief, G. Foti, T. Frederiksen, D. Sanchez-Portal, a. Arnau, J. P. Nys, P. Leclère, D. Vuillaume and N. Clément, *Nanoscale*, 2015, **7**, 1809–1819.
5 S. Ma, S. Zheng, D. Cao and H. Guo, *Particuology*, 2010, **8**, 468–472.
6 N. Xu, M. Zhang, W. Li, G. Zhao, X. Wang and W. Liu, *Wear*, 2013, **307**, 35–43.
7 Q. Xue, W. Liu and Z. Zhang, *Wear*, 1997, **213**, 29–32.
8 H. Etemadi, a. Shojaei and P. Jahanmard, *J. Reinf. Plast. Compos.*, 2014, **33**, 166–178.
9 M. M. Saatchi and a. Shojaei, *Mater. Sci. Eng. A*, 2011, **528**, 7161–7172.
10 A. a. Alazemi, V. Etacheri, A. D. Dysart, L.-E. Stacke, V. G. Pol and F. Sadeghi, *ACS Appl. Mater. Interfaces*, 2015, 150225103255004.
11 D. Kim and L. a Archer, *Langmuir*, 2011, **27**, 3083–94.
12 X. Li, Z. Cao, Z. Zhang and H. Dang, *Appl. Surf. Sci.*, 2006, **252**, 7856–7861.
13 T. Jiang, T. Kuila, N. H. Kim, B. C. Ku and J. H. Lee, *Compos. Sci. Technol.*, 2013, **79**, 115–125.
14 S. G. Vilt, N. Martin, C. McCabe and G. Kane Jennings, *Tribol. Int.*, 2011, **44**, 180–186.
15 E. Amerio, P. Fabbri, G. Malucelli, M. Messori, M. Sangermano and R. Taurino, *Prog. Org. Coatings*, 2008, **62**, 129–133.
16 Y. Kang, X. Chen, S. Song, L. Yu and P. Zhang, *Appl. Surf. Sci.*, 2012, **258**, 6384–6390.
17 S. Song, R. Chu, J. Zhou, S. Yang and J. Zhang, *J. Phys. Chem. C*, 2008, **112**, 3805–3810.
18 R. P. Bagwe, L. R. Hilliard and W. Tan, *Langmuir*, 2006, **22**, 4357–4362.
19 T. Iwano and K. Kobayashi, *IEEE Trans. Magn.*, 2005, **41**, 3010–3012.
20 R. L. Jones, B. L. Harrod and J. D. Batteas, *Langmuir*, 2010, **26**, 16355–16361.
21 Y.-C. Chen, H.-C. Lin and Y.-D. Lee, *J. Polym. Res.*, 2004, **11**, 1–7.
22 Y. Gao, G. Chen, Y. Oli, Z. Zhang and Q. Xue, *Wear*, 2002, **252**, 454–458.

23 V. Jaiswal, R. B. Rastogi, R. Kumar, L. Singh and K. D. Mandal, *J. Mater. Chem. A*, 2014, **2**, 375–386.
24 B. Yu, L. Qian, J. Yu and Z. Zhou, *Tribol. Lett.*, 2008, **34**, 1–10.
25 A. C. Hervé, J. J. Yaouanc, J. C. Clément, H. des Abbayes and L. Toupet, *J. Organomet. Chem.*, 2002, **664**, 214–222.
26 L. Chang, Z. Zhang, L. Ye and K. Friedrich, *Wear*, 2007, **262**, 699–706.
27 R. Bosman and D. J. Schipper, *Tribol. Lett.*, 2011, **41**, 263–282.

Effects of functional group on the tribological properties of hairy silica nanoparticles as an additive to polyalphaolefin

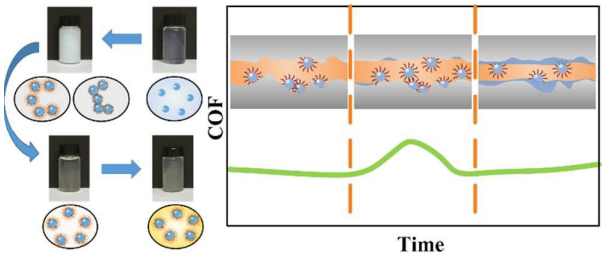

Hairy silica nanoparticles with different kinds of functional groups were prepared and dispersed into Polyalphaolefin by a four step process, the effect of functional groups on the tribological properties of hairy silica nanoparticles were investigated.